Assisted Self-Assembly to Target Heterometallic Mn-Nd and Mn-Sm SMMs: Synthesis and Magnetic Characterisation of [Mn 7 Ln 3 (O) 4 (OH) 4 (mdea) 3 (piv) 9 (NO 3) 3] (Ln=Nd, Sm, Eu, Gd)**

Hagen Kaemmerer, Valeriu Mereacre, Ayuk M Ako, Samir Mameri, Christopher E Anson, Rodolphe Clérac, Annie K Powell

Assisted Self-Assembly to Target Heterometallic Mn-Nd and Mn-Sm SMMs: Synthesis and Magnetic Characterisation of $[Mn_7Ln_3(O)_4(OH)_4(mdea)_3(piv)_9(NO_3)_3]$ (Ln = Nd, Sm, Eu, Gd)**

Hagen Kaemmerer,[a, b] Valeriu Mereacre,*[a] Ayuk M. Ako,[a] Samir Mameri,[c] Christopher E. Anson,[a] Rodolphe Clérac,*[d] and Annie K. Powell*[a, b, e]

Abstract: In an assisted self-assembly approach starting from the $[Mn_6O_2(piv)_{10}(4\text{-Me-py})_2(pivH)_2]$ cluster a family of Mn–Ln compounds (Ln = Pr–Yb) was synthesised. The reaction of $[Mn_6O_2(piv)_{10}(4\text{-Me-py})_2(pivH)_2]$ (**1**) with *N*-methyldiethanolamine ($mdeaH_2$) and $Ln(NO_3)_3 \cdot 6H_2O$ in MeCN generally yields two main structure types: for Ln = Tb–Yb a previously reported Mn_5Ln_4 motif is obtained, whereas for Ln = Pr–Eu a series of Mn_7Ln_3 clusters is obtained. Within this series the Gd^{III} analogue represents a special case because it shows both structural types as well as a third Mn_2Ln_2 inverse butterfly motif. Variation in reaction conditions allows access to different structure types across the whole series. This prompts further studies into the reaction mechanism of this cluster assisted self-assembly approach. For the Mn_7Ln_3 analogues reported here variable-temperature magnetic susceptibility measurements suggest that antiferromagnetic interactions between the spin carriers are dominant. Compounds incorporating $Ln = Nd^{III}$(**2**), Sm^{III}(**3**) and Gd^{III} (**5**) display SMM behaviour. The slow relaxation of the magnetisation for these compounds was confirmed by ac measurements above 1.8 K.

Introduction

In the 1990's efforts in the synthesis of **3d**–**4f** coordination compounds were mostly concentrated on Cu–Gd systems which predominantly are ferromagnetically coupled and generate high spin ground states, but show minor magnetic anisotropy. Along this line, in recent times, the new approaches of combining **3d** and **4f** metals ions have produced a huge number of heteronuclear **4f**-based systems incorporating Cr^{III},[1] Fe^{III},[2] Co^{II},[3] Ni^{II},[4] and Cu^{II}.[5] There is increasing research in developing synthetic routes towards magnetic clusters with high blocking temperatures. In spite of the fact that many heteropolynuclear SMMs (Single Molecule Magnet) are now known, a greater part of them represent complexes containing the high spin Mn^{III} ion, which has large uniaxial anisotropy.[6] Due to the fact that lanthanide ions can exhibit even higher magnetic moments and generally larger single-ion anisotropy, an approach that progressively is gaining ground is the combination of transition metal ions with lanthanide ions.[1–5] By merging **3d** and **4f** magnetic carriers together with suitable bridging ligands into a single molecule, very large magnetic moments and uniaxial anisotropy can be achieved. Although

[a] *H. Kaemmerer, Dr. V. Mereacre, Dr. A. M. Ako, Dr. C. E. Anson, Prof. A. K. Powell*
Institute of Inorganic Chemistry
Karlsruhe Institute of Technology
Engesserstr. 15, 76131 Karlsruhe (Germany)
E-mail: valeriu.mereacre@kit.edu
annie.powell@kit.edu

[b] *H. Kaemmerer, Prof. A. K. Powell*
Institute for Quantum Materials and Technologies (IQMT)
Karlsruhe Institute of Technology
Hermann-von-Helmholtz-Platz 1
76344 Eggenstein-Leopoldshafen (Germany)

[c] *Dr. S. Mameri*
Université de Strasbourg
IUT Robert Schuman
CS 10315, 67411 Illkirch Cedex (France)

[d] *Dr. R. Clérac*
Univ. Bordeaux
CNRS, Centre de Recherche Paul Pascal
UMR 5031, 33600 Pessac (France)
E-mail: clerac@crpp-bordeaux.cnrs.fr

[e] *Prof. A. K. Powell*
Institute for Nanotechnology (INT)
Karlsruhe Institute of Technology
Hermann-von-Helmholtz-Platz 1
76344 Eggenstein-Leopoldshafen (Germany)

[**] *SMMs = single molecule magnets, $mdeaH_2$ = N*-methyldiethanolamine, pivH = pivalic acid.

the **3d**–**4f** superexchange is weak in comparison with that for **3d**–**3d** ions, the large dipolar contribution of the **4f** ions can suppress zero-field quantum tunnelling of magnetisation (QTM) and gives rise to a more complex, multilevel exchange type barrier.[1b]

One particular synthetic strategy has been to use certain preformed coordination clusters[7] to manipulate the kinetics of reactions and introduce co-ligands into the reaction.[2j,l] This attempt at steering the seemingly serendipitous nature[8] of the coordination cluster synthesis can be described as a cluster assisted self-assembly. The partial disassembly of the **3d** metal cluster in situ limits the availability of certain components and allows metastable species to be isolated.

Results and Discussion

Previously, we reported the synthesis, crystal structures and magnetic properties of high nuclearity heterometallic $[Mn_5Ln_4(O)_6(mdea)_2(mdeaH)_2(piv)_6(NO_3)_4(H_2O)_2]\cdot 2MeCN$ (Ln = Tb^{III}, Dy^{III}, Ho^{III}, Y^{III}) coordination cluster compounds.[6k] All of them showed ac signals consistent with SMM behaviour with the $[Mn_5Dy_4]$ analogue exhibiting hysteresis loops at low temperature. These results prompted us to extend this work to the lighter Ln^{III} ions left of Tb^{III}. The reaction of $[Mn_6O_2(piv)_{10}(4\text{-Me-py})_{2.5}(pivH)_{1.5}]$[7d] (**1**) with *N*-methyldiethanolamine ($mdeaH_2$) and $Ln(NO_3)_3\cdot 6H_2O$ in 1:10:6 molar ratio in MeCN gave a brown solution from which dark-brown crystals of $[Mn_7Ln_3(O)_4(OH)_4(mdea)_3(piv)_9(NO_3)_3]\cdot 3MeCN$ (Ln = Nd^{III} (**2**), Sm^{III} (**3**), Eu^{III} (**4**), Gd^{III} (**5**)), complexes were obtained after one week. (Figure 1) Crystallisation of the Gd^{III} analogue (**5**) was found not to be trivial. To obtain the pure $[Mn_7Gd_3]$ complex the second crop of crystals have to be isolated within one week. Otherwise, if the solution is left to stand for a longer time, a mixture of three types of products of obtained: Mn_7Gd_3 (**5**), a Mn_5Gd_4 cluster (**6**) isostructural with the reported Mn_5Ln_4 series[6k]) and an "inverse butterfly type" Mn_2Gd_2 cluster (**7**) (Figure 2).

With such large cluster systems, it is often the case that the same core topology cannot be obtained for all lanthanides, in consequence of the significant variation in the size of Ln^{III} ions across the lanthanide series – the lanthanide contraction. In the present case, the Gd^{III} ion is at the border between Mn_7Ln_3 and Mn_5Ln_4 series. Such cases are not unprecedented. For example, recently we reported several series: Mn_2Ln_2[9] (Ln = La–Nd) and Mn_2Ln_3[10] (Ln = Tb–Er) for which no Gd^{III} species was possible to produce although the reaction conditions were the same. We

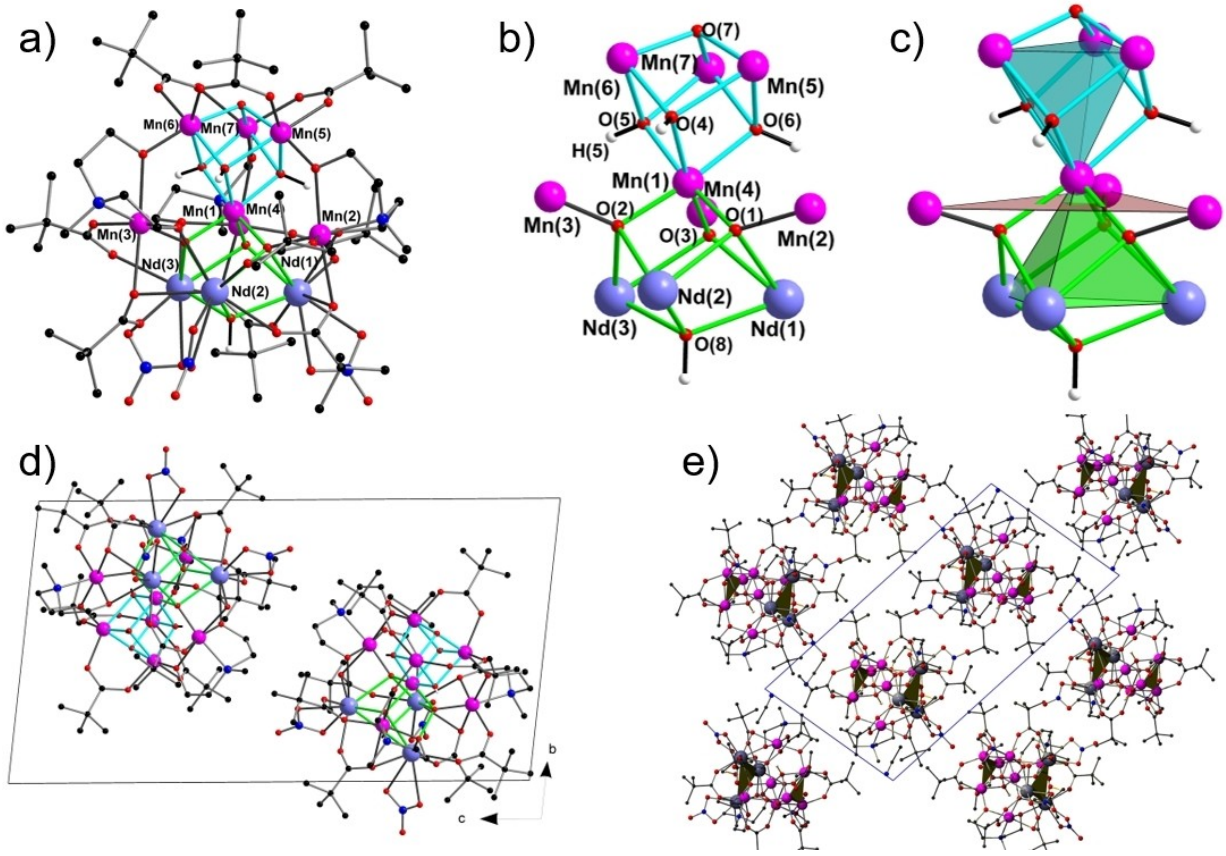

Figure 1. (a) Molecular structure and (b) core of **2**. The green and light blue bonds emphasise the $MnNd_3$ and Mn_4 cubane units. Organic H atoms are omitted for clarity. Nd blue grey; Mn^{III} pink; O red; N blue; C black, H white. (c) Core represented by two tetrahedra, Mn_4 and $MnNd_3$, sharing one vertex and a plane of peripheral Mn^{III} ions. (d) Unit cell representation for **2** along the *a* axes. Organic H atoms are omitted for clarity. (e) Packing arrangement along the b axes. Brown planes are Mn_3 and Nd_3 parallel planes of every cubane, respectively.

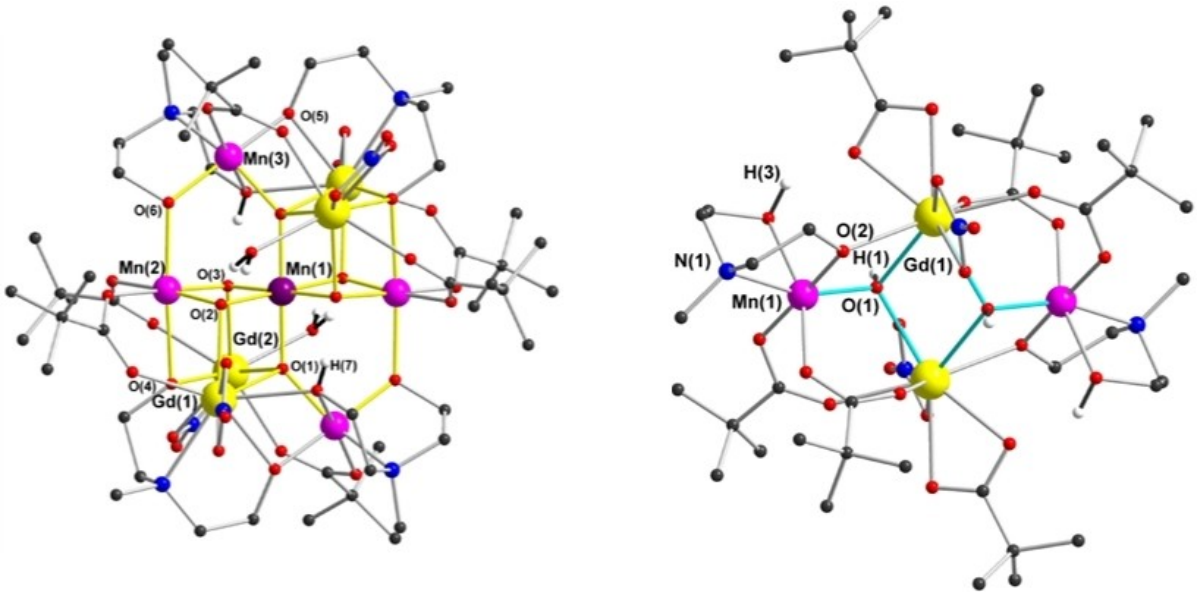

Figure 2. Molecular structure of $[Mn_5Gd_4(O)_6(mdea)_2(mdeaH)_2(piv)_6(NO_3)_4(H_2O)_2]\cdot 2MeCN$ (**6**) (left) and $[Mn_2Gd_2(OH)_2(mdeaH)_2(piv)_6(NO_3)_2]\cdot MeCN$ (**7**) (right). Organic H atoms are omitted for clarity. Gd yellow; Mn^{III} pink; Mn^{IV} purple; O red; N blue; C black; H white

also found out that for a Mn_5Ln_8[11] series (Ln = Pr, Nd, Sm, Gd, Tb), carrying out the reactions under similar conditions with $Ce^{III}(NO_3)_3\cdot 6H_2O$ or $La^{III}(NO_3)_3\cdot 6H_2O$ resulted in the formation of the aggregates $[Ce^{IV}_6Ce^{III}_2Mn^{III}_2(t\text{-bdea})_2(piv)_{12}(NO_3)_2(OAc)_2]$[12] and $[Mn^{III}_4La_4(\mu_3\text{-}OH)_4(\mu\text{-}NO_3)_4(piv)_8(t\text{-bdea})_4]$,[13] respectively.

Although the starting manganese source $[Mn_6]$ (**1**) is a mixed-valent cluster with four Mn^{II} and two Mn^{III} ions, this is not the case in the final homovalent $Mn^{III}_7Ln_3$ product. The same situation was observed in the $[Mn_5Ln_4]$ series where the $[Mn_5Ln_4]$ cation is mixed-valent, but now with four Mn^{III} and one Mn^{IV}. Clearly, the formation of all compounds in these two series involve not just complicated fragmentation and aggregation steps, but also redox chemistry of the Mn. Thus, there are likely many Mn_x and Mn_xLn_y species in equilibrium in solution, and the exact species that preferentially crystallises, $[Mn_7Ln_3]$ or $[Mn_5Ln_4]$, is dictated by relative solubilities, crystallisation time and kinetics, and the Ln^{III} ionic radius.

Although complexes **2** and **5** crystallise in the triclinic space group *P*-1, while complexes **3** and **4** crystallise in the monoclinic space group $P2_1/n$ (Table 1), the clusters in all four compounds are isostructural, and that of **2** is described here as a representative example for the series. The molecular structure of **2** is shown in Figure 1a, with the core of the cluster in Figure 1b, and has idealised threefold rotational symmetry. The $\{Mn_7Nd_3(\mu_4\text{-}O)_3(\mu_3\text{-}O)(\mu_3\text{-}OH)_3\}^{10+}$ core can be viewed as being comprised of homometallic $Mn_4^{III}(O)(OH)_3$ and heterometallic $Mn^{III}Nd_3(O)_3(OH)$ cubane units sharing a common Mn^{III} vertex, Mn(1), with the three oxido bridges in the $Mn^{III}Nd_3(O)_3(OH)$ cubane each additionally coordinating to a further "outer" Mn^{III} centre, Mn(5), Mn(6) and Mn(7). Each of these outer Mn is chelated by a doubly-deprotonated $(mdea)^{2-}$ ligand; in each case one of the alkoxo arms bridges to a Nd^{III}, the other to a Mn^{III} in the $Mn_4^{III}(O)(OH)_3$ cubane. Additional bridging is provided by the 15 pivalate ligands, with each Nd chelated by a nitrate ligand. The Mn^{III} oxidation states and the deprotonation levels of the oxido and hydroxide bridges were established by bond valence sum calculations,[14] and the observation of Jahn-Teller elongation axes for each Mn^{III}. For the three outer Mn^{III}, these axes are those defined by the coordination of the $(mdea)^{2-}$ ligand oxygens, and are thus close to co-parallel to the molecular three-fold axis. For Mn(2), Mn(3) and Mn(4), the axes are each defined by a (μ_3-OH) and a pivalate oxygen, with the three such axes forming a propeller arrangement about the molecular threefold axes. Perhaps surprisingly, one of the three possible orientations for the Jahn-Teller axis of the central Mn^{III}, Mn(1), that involving O(2) and O(7), has been selected over the other two in the crystal structure, resulting in a deviation from the idealised threefold symmetry. The Nd^{III} ions are each nine-coordinate with a coordination polyhedron that may best be described as a distorted tricapped trigonal prism. The temperature dependence of the magnetic susceptibility χT for the Mn_7Ln_3 compounds **2**–**5** under a 0.1 T applied field are shown in Figure 3 and summarised in Table 2. The observed values at 300 K are in reasonable agreement with those calculated for seven isolated Mn^{III} and three Ln^{III} ions, with the exception of **4**, where the observed value is rather higher than the calculated, resulting from thermal population of magnetic excited states in the nominally-diamagnetic Eu^{III} ions. The χT versus T plots of Mn_7Nd_3 (**2**), Mn_7Sm_3 (**3**) and Mn_7Eu_3 (**4**) show rather similar profiles, where the χT value remains almost constant from 300 K down to ca. 150 K, and then decreases continuously upon lowering the temperature. Such behaviour indicates that the susceptibilities of these three compounds are dominated by antiferromagnetic (AF) interactions between the seven Mn^{III}

Table 1. Crystallographic data for compounds **2–4** and **6–8**.[a]

	2	**3**	**4**	**6**	**7**	**8**
formula	$C_{66}H_{127}Mn_7N_9Nd_3O_{41}$	$C_{66}H_{127}Mn_7N_9Sm_3O_{41}$	$C_{66}H_{127}Mn_7N_9Eu_3O_{41}$	$C_{54}H_{110}Mn_5N_{10}Gd_4O_{40}$	$C_{42}H_{83}Mn_2N_5Gd_2O_{24}$	$C_{44}H_{86}Mn_2N_6Pr_2O_{24}$
Mr [g mol^{-1}]	2520.07	2538.37	2543.23	2443.22	1466.51	1474.88
crystal system	triclinic	monoclinic	monoclinic	monoclinic	monoclinic	monoclinic
space group	$P\bar{1}$	$P2_1/n$	$P2_1/n$	$P\bar{1}$	$P\bar{1}$	$P\bar{1}$
a [Å]	14.3815(11)	22.0593(10)	22.2719(13)	13.8365(7)	10.9664(7)	10.9078(4)
b [Å]	15.0511(11)	18.4408(8)	18.6189(10)	14.0026(7)	14.0196(9)	13.3251(5)
c [Å]	25.8828(19)	24.1213(11)	24.3325(14)	14.0996(7)	21.8482(14)	13.7408(5)
α [°]	91.889(1)	90	90	107.760(1)	78.567(5)	100.104(3)
β [°]	100.900(1)	95.685(1)	95.658(1)	110.155(1)	79.212(5)	112.766(3)
γ [°]	111.755(1)	90	90	109.090(1)	68.444(5)	111.712(3)
V [Å^3]	5076.9(7)	9764.1(8)	10041.0(10)	2137.93(19)	3037.2	1588.23(11)
Z	2	4	4	1	2	1
ρ_{calcd} [g cm^{-3}]	1.649	1.725	1.682	1.898	1.603	1.542
μ [mm^{-1}]	2.426	2.732	2.776	3.858	2.637	10.584
F(000)	2538	5088	5112	1205	1480	752
T [K]	100	100	100	100	150	150
measured reflections	26251	54229	48877	12958	20833	17638
unique reflections	19657	21971	21988	9049	12451	7480
R_{int}	0.0536	0.0520	0.0757	0.0130	0.0303	0.0390
reflns with I > 2σ(I)	12696	16630	16458	7963	10044	7103
refined parameters	1135	1198	1227	521	724	369
R_1 [I > 2σ(I)]	0.0854	0.0400	0.0516	0.0231	0.0365	0.0497
S (all data)	1.062	0.948	0.980	0.976	0.955	1.054
wR_2 (all data)	0.2048	0.0715	0.1363	0.0543	0.0942	0.1364
CCDC no	2101902	2101903	2101900	2101901	2101899	2101904

[a] For compounds **5** and **9**, comparison of unit cell measurements (Table S1) with those in this Table confirmed the identity of the compounds

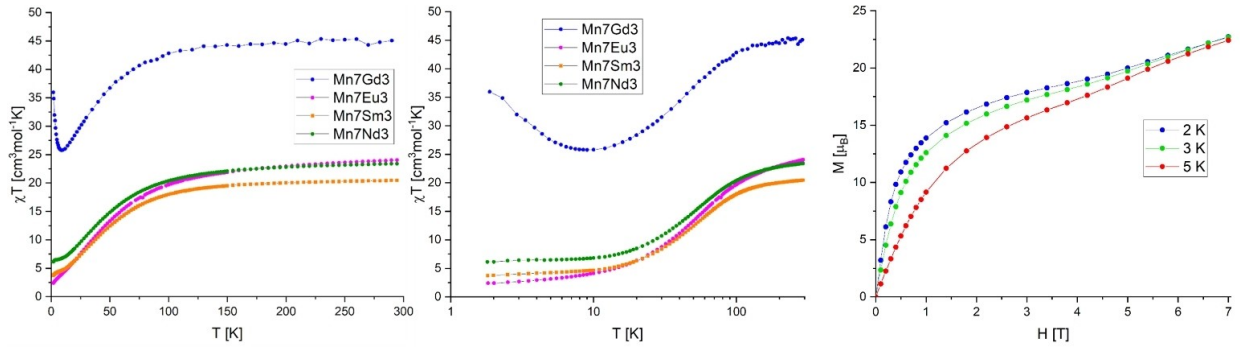

Figure 3. Temperature dependence of the χT product (left) and its semi log-plot (centre) for polycrystalline samples of Mn_7Nd_3 (**2**), Mn_7Sm_3 (**3**), Mn_7Eu_3 (**4**) and Mn_7Gd_3 (**5**) at 0.1 T; field-dependence of the magnetisation for **5** (right)

Table 2. Observed and calculated magnetic moments for **2–5** at 300 and 1.8 K

Complex	#	C (Ln^{III})	g_j (Ln^{III})	χT at 300 K	χT_{calcd}	χT at 1.8 K
Mn_7Nd_3	**2**	1.64	8/11	23.4	25.9	6.13
Mn_7Sm_3	**3**	0.09	2/7	19.2	20.5	3.72
Mn_7Eu_3	**4**	0 (at low T)	0	24.1	21.0	2.25
Mn_7Gd_3	**5**	7.875	2	45.0	44.6	36.0

centres. Furthermore, for these three compounds, the χT products each seem to have reached limiting values at 1.8 K suggesting that at this low temperature each has a well-defined spin ground state. The extrapolation of the χT products for Mn_7Sm_3 (**3**) and Mn_7Eu_3 (**4**) to 2.8 and 2.5 cm^3 K mol^{-1}, respectively, suggests a spin-ground state of $S = 2$ for the Mn^{III}_7 moiety, given that Eu^{III} is diamagnetic at low temperature, while Sm^{III}, with C = 0.09 cm^3 K mol^{-1}, is close to non-magnetic. Given that all the Mn–O–Mn angles between the three outer Mn^{III} and those in the Mn^{III}_4 cubane unit are all rather obtuse (124–126°), while those within the cubane are much closer to 90°, a reasonable rationalisation of this $S = 2$ state would involve a ferromagnetic arrangement of the four Mn^{III} within the cubane, but with the three outer Mn^{III} spins all antiparallel to them, leaving one Mn^{III} spin uncompensated.

The corresponding curve for the Mn_7Gd_3 analogue (**5**) shows a rather similar profile down to ca. 15 K, but then, unlike the others, it rises sharply, reaching 36.0 cm^3 K mol^{-1} at 1.8 K. From the semi log-plot in Figure 3 (centre), the limiting low temperature value is ca. 40 cm^3 K mol^{-1}, which would correspond to a spin-ground state of $S = 17/2$. This can readily be rationalised in terms of a ferromagnetically coupled Gd^{III}_3 triangle (with S = 21/2), to which the residual S = 4/2 spin from the Mn_7 unit is

coupled antiferromagnetically. Interestingly, the magnetisation curve for (**5**) shows an inflection point at ca. 18 μ_B for a field of ca. 3.5 T, above which the magnetisation begins to rise again. This indicates that above this field an excited state with higher *S* (probably that with the $S=2$ Mn_7 spin now flipped to be parallel to those of the three Gd^{III} giving $S=25/2$) is being populated by the higher fields.

To probe the slow relaxation of magnetisation, ac susceptibility measurements under zero applied dc field were carried out on all four Mn_7Ln_3 complexes. While Mn_7Eu_3 (**4**) does not exhibit any out-of-phase ac signal, complexes **2**, **3** and **5** display frequency-dependent in-phase χ' and out-of-phase χ'' signals, indicative of slow magnetic relaxation and potential SMM behaviour (Figure 4). The Mn_7Gd_3 compound **5** displays out-of-phase χ'' signals below 3 K, but without visible maxima above 1.8 K. This indicates that the Mn^{III}_7 moiety of the clusters has a negative but small axial anisotropy D, which when combined with the low $S_T=2$ ground state in **4** does not result in a barrier U_{eff} sufficient to give observable slow relaxation at 1.8 K. However, replacement of the three Eu^{III} in **4** by the three ferromagnetically-coupled Gd^{III} in **5** increases S_T for the latter cluster to 17/2 and in principle (assuming D is unchanged) increases U_{eff} by a factor of ca. 18, now resulting in observable slow relaxation, but without maxima at zero dc field. By contrast, compounds **2** and **3** each display out-of-phase χ'' signals with maxima above 2.0 K. The corresponding energy barriers could be calculated by fitting the data to an Arrhenius equation ($\tau=\tau_0 \exp(U_{eff}/kT)$), which resulted in $U_{eff}/k_B=27.4$ and 13.4 K ($\tau_0=3.6\times10^{-9}$ and 2.1×10^{-7} s) for **2** and **3**, respectively (Figure S4). **2** and **3** are thus new additions to the rather small number of Mn-4f SMMs involving the lighter lanthanides so far reported in the literature. Comparing the out-of-phase data for **2** and **3** with those for **5**, it is clear that a large part of the SMM behaviour of **2** and **3** results from the anisotropy contributed by the Nd_3 and Sm_3 triangles. It is also of interest to note the inverse relationship in terms of their anisotropy ellipsoids between Nd and Er and between Sm and Dy, see Figure S6.

Conclusion

In summary, we have presented a new family of high-nuclearity Mn-4f compounds, representing the second series of *N*-methyldiethanolamine and pivalic acid based [Mn–Ln] heterometallic complexes. Three compounds, **2**, **3** and **5**, show evidence of SMM behaviour. The slow relaxation of the magnetisation for these compounds was confirmed by *ac* measurements above 1.8 K. For **2** and **3** well-defined *ac* signals could be observed and the values for U_{eff} of 27.4 and 13.4 K, respectively, confirming that these compounds are rare examples of Mn–Nd and Mn–Sm-based SMMs.

The series of molecular species reported in this paper highlight the importance of chemical approaches to obtain targeted series of pure molecular species showing interesting magnetic properties. Although much of the published research based on combinations of manganese and lanthanides has concentrated on the heavier lanthanides, the work presented here shows that incorporation of lighter lanthanides can also lead to aesthetically pleasant and magnetically interesting compounds. Additionally, the present system is an example for the complexity of coordination chemistry synthesis. We previously suggested that the system shows a clear break in the lanthanide series around Gd^{III} since we found different structures for the same synthesis method for Gd^{III} first. As it turns out investigating the purification of the Mn_7Gd_3 synthesis led to the realisation that the system is in fact more complicated. It seems that all 3 known structure types could be present in solution but it depends on the kinetics of the reaction conditions as to whether the Mn_5Ln_4 or the Mn_7Ln_3 series (or both) crystallises, while the Mn_2Ln_2 system seems to

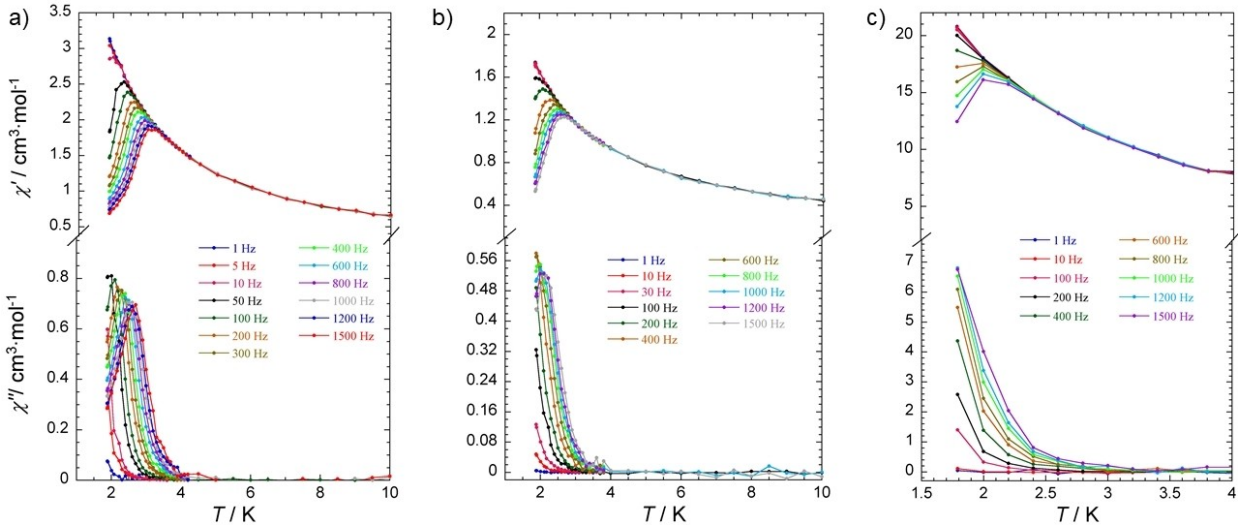

Figure 4. Temperature dependence of the in-phase (χ') and the out-of-phase (χ'') ac susceptibility components at different frequencies for Mn_7Nd_3 **2** (a), Mn_7Sm_3 **3** (b) and Mn_7Gd_3 **5** (c) under zero applied dc field.

be the thermodynamic end point of the reaction, as this motif was found for various lanthanides across the series.

These types of reactions could potentially be decrypted using artificial intelligence (AI) in conjunction with machine learning, both of which are now high interest topics in coordination chemistry.[15] For example, Cronin et al. have been able to show that using AI and robotics can successfully predict reaction products and optimise reaction conditions for certain organic synthesis as well as that of polyoxometallates.[16] To apply these new techniques to these complex coordination chemistry synthesis promises to be an exciting research area.

Experimental Section

Experimental details are discussed in the Supporting Information.

Crystallography

X-ray data for **2–7** were collected at 100 K on a Bruker SMART Apex CCD diffractometer using a Mo-K_α rotating anode source. Data for **8** and **9** were collected at 150 K on a Stoe STADIVARI diffractometer with a Dectris Eiger2 R4 M detector using a Metaljet2 Ga-K_α source. Data were corrected for absorption, Lorentz and polarisation factors. The structure determination and refinement were performed using SHELXT[18] and SHELXL[19] within OLEX2.[20] Figures were produced using the program Diamond 4.1.

Unit cell data and details of the structure refinements for compounds **2–8** are listed in Table 1. Deposition Numbers 2101899 (for **7**), 2101900 (for **4**), 2101901 (for **6**), 2101902 (for **2**), 2101903 (for **3**), and 2101904 (for **8**) contain the supplementary crystallographic data for this paper. These data are provided free of charge by the joint Cambridge Crystallographic Data Centre and Fachinformationszentrum Karlsruhe Access Structures service.

Magnetic measurements

The magnetic susceptibility measurements were carried out using a Quantum Design SQUID magnetometer MPMS-XL on polycrystalline samples of 16.76 mg, 18.14 mg, 17.20 mg and 2.9 mg for Mn_7Nd_3 (**2**), Mn_7Sm_3 (**3**), Mn_7Eu_3 (**4**) and Mn_7Gd_3 (**5**) respectively. ac susceptibility measurements were made with an oscillating ac field of 3 Oe and ac frequencies ranging from 1 to 1500 Hz. *M* vs. *H* measurements were performed at 100 K to check for the presence of ferromagnetic impurities that have been found to be absent. The magnetic data were corrected for the sample holder, the mineral oil and the diamagnetic contribution.

Acknowledgements

We thank the DFG SFB/TRR88 "3MET" and the Helmholtz POF STN for financial support. VM acknowledges the support from Alexander von Humboldt Foundation. RC thank the CNRS, the University of Bordeaux, the Région Nouvelle Aquitaine, the GdR MCM-2: Magnétisme & Commutation Moléculaires, and Quantum Matter Bordeaux. Open Access funding enabled and organized by Projekt DEAL.

[1] a) T. Birk, K. S. Pedersen, C. A. Thuesen, T. Weyhermüller, M. Schau-Magnussen, S. Piligkos, H. Weihe, S. Mossin, M. Evangelisti, J. Bendix, *Inorg. Chem.* **2012**, *51*, 5435–5443; b) S. K. Langley, D. P. Wielechowski, V. Vieru, N. F. Chilton, B. Moubaraki, B. F. Abrahams, L. F. Chibotaru, K. S. Murray, *Angew. Chem. Int. Ed.* **2013**, *52*, 12014–12019; *Angew. Chem.* **2013**, *125*, 12236–12241; c) A. McRobbie, A. R. Sarwar, S. Yeninas, H. Nowell, M. L. Baker, D. Allan, M. Luban, C. A. Muryn, R. G. Pritchard, R. Prozorov, G. A. Timco, F. Tuna, G. F. S. Whitehead, R. E. P. Winpenny, *Chem. Commun.* **2011**, *47*, 6251–6253; d) J. Rinck, G. Novitchi, W. Van den Heuvel, L. Ungur, Y. Lan, W. Wernsdorfer, C. E. Anson, L. F. Chibotaru, A. K. Powell, *Angew. Chem. Int. Ed.* **2010**, *49*, 7583–7587; *Angew. Chem.* **2010**, *122*, 7746–7750; e) C. A. Thuesen, K. S. Pedersen, M. Schau-Magnussen, M. Evangelisti, J. Vibenholt, S. Piligkos, H. Weihe, J. Bendix, *Dalton Trans.* **2012**, *41*, 11284–11292; f) H. Xiang, W.-G. Lu, W.-X. Zhang, L. Jiang, *Dalton Trans.* **2013**, *42*, 867–870.

[2] a) G. Abbas, Y. Lan, V. Mereacre, G. Buth, M. T. Sougrati, F. Grandjean, G. J. Long, C. E. Anson, A. K. Powell, *Inorg. Chem.* **2013**, *52*, 11767–11777; b) G. Abbas, Y. Lan, V. Mereacre, W. Wernsdorfer, R. Clérac, G. Buth, M. T. Sougrati, F. Grandjean, G. J. Long, C. E. Anson, A. K. Powell, *Inorg. Chem.* **2009**, *48*, 9345–9355; c) M. N. Akhtar, V. Mereacre, G. Novitchi, J.-P. Tuchagues, C. E. Anson, A. K. Powell, *Chem. Eur. J.* **2009**, *15*, 7278–7282; d) A. M. Ako, V. Mereacre, R. Clérac, I. J. Hewitt, Y. Lan, C. E. Anson, A. K. Powell, *Dalton Trans.* **2007**, 5245–5247; e) A. Baniodeh, I. J. Hewitt, V. Mereacre, Y. Lan, G. Novitchi, C. E. Anson, A. K. Powell, *Dalton Trans.* **2011**, *40*, 4080–4086; f) J. Bartolomé, G. Filoti, V. Kuncser, G. Schinteie, V. Mereacre, C. E. Anson, A. K. Powell, D. Prodius, C. Turta, *Phys. Rev. B* **2009**, *80*, 014430; g) J.-P. Costes, F. Dahan, F. Dumestre, J. Modesto Clemente-Juan, J. Garcia-Tojal, J.-P. Tuchagues, *Dalton Trans.* **2003**, 464–468; h) M. Ferbinteanu, T. Kajiwara, K.-Y. Choi, H. Nojiri, A. Nakamoto, N. Kojima, F. Cimpoesu, Y. Fujimura, S. Takaishi, M. Yamashita, *J. Am. Chem. Soc.* **2006**, *128*, 9008–9009; i) A. Figuerola, J. Ribas, M. Llunell, D. Casanova, M. Maestro, S. Alvarez, C. Diaz, *Inorg. Chem.* **2005**, *44*, 6939–6948; j) H. Kaemmerer, A. Baniodeh, Y. Peng, E. Moreno-Pineda, M. Schulze, C. E. Anson, W. Wernsdorfer, J. Schnack, A. K. Powell, *J. Am. Chem. Soc.* **2020**, *142*, 14838–14842; k) V. Mereacre, *Angew. Chem. Int. Ed.* **2012**, *51*, 9922–9925; *Angew. Chem.* **2012**, *124*, 10060–10063; l) V. Mereacre, A. Baniodeh, C. E. Anson, A. K. Powell, *J. Am. Chem. Soc.* **2011**, *133*, 15335–15337; m) V. Mereacre, D. Prodius, Y. Lan, C. Turta, C. E. Anson, A. K. Powell, *Chem. Eur. J.* **2011**, *17*, 123–128; n) M. Murugesu, A. Mishra, W. Wernsdorfer, K. A. Abboud, G. Christou, *Polyhedron* **2006**, *25*, 613–625; o) I. Nemec, M. Machata, R. Herchel, R. Boča, Z. Trávníček, *Dalton Trans.* **2012**, *41*, 14603–14610; p) F. Pointillart, K. Bernot, R. Sessoli, D. Gatteschi, *Chem. Eur. J.* **2007**, *13*, 1602–1609; q) S. Schmidt, D. Prodius, V. Mereacre, G. E. Kostakis, A. K. Powell, *Chem. Commun.* **2013**, *49*, 1696–1698; r) D. Schray, G. Abbas, Y. Lan, V. Mereacre, A. Sundt, J. Dreiser, O. Waldmann, G. E. Kostakis, C. E. Anson, A. K. Powell, *Angew. Chem. Int. Ed.* **2010**, *49*, 5185–5188; *Angew. Chem.* **2010**, *122*, 5312–5315; s) S. A. Stoian, C. Paraschiv, N. Kiritsakas, F. Lloret, E. Münck, E. L. Bominaar, M. Andruh, *Inorg. Chem.* **2010**, *49*, 3387–3401; t) H. Xiang, V. Mereacre, Y. Lan, T.-B. Lu, C. E. Anson, A. K. Powell, *Chem. Commun.* **2013**, *49*, 7385–7387; u) T. Yamaguchi, J.-P. Costes, Y. Kishima, M. Kojima, Y. Sunatsuki, N. Bréfuel, J.-P. Tuchagues, L. Vendier, W. Wernsdorfer, *Inorg. Chem.* **2010**, *49*, 9125–9135; v) Y.-F. Zeng, G.-C. Xu, X. Hu, Z. Chen, X.-H. Bu, S. Gao, E. C. Sañudo, *Inorg. Chem.* **2010**, *49*, 9734–9736.

[3] a) V. Chandrasekhar, B. M. Pandian, R. Azhakar, J. J. Vittal, R. Clérac, *Inorg. Chem.* **2007**, *46*, 5140–5142; b) K. C. Mondal, A. Sundt, Y. Lan, G. E. Kostakis, O. Waldmann, L. Ungur, L. F. Chibotaru, C. E. Anson, A. K. Powell, *Angew. Chem. Int. Ed.* **2012**, *51*, 7550–7554; *Angew. Chem.* **2012**, *124*, 7668–7672; c) J.-B. Peng, Q.-C. Zhang, X.-J. Kong, Y.-Z. Zheng, Y.-P. Ren, L.-S. Long, R.-B. Huang, L.-S. Zheng, Z. Zheng, *J. Am. Chem. Soc.* **2012**, *134*, 3314–3317; d) L.-F. Zou, L. Zhao, Y.-N. Guo, G.-M. Yu, Y. Guo, J. Tang, Y.-H. Li, *Chem. Commun.* **2011**, *47*, 8659–8661.

[4] a) V. Chandrasekhar, B. M. Pandian, R. Boomishankar, A. Steiner, J. J. Vittal, A. Houri, R. Clérac, *Inorg. Chem.* **2008**, *47*, 4918–4929; b) C. G.

Efthymiou, T. C. Stamatatos, C. Papatriantafyllopoulou, A. J. Tasiopoulos, W. Wernsdorfer, S. P. Perlepes, G. Christou, *Inorg. Chem.* **2010**, *49*, 9737–9739; c) M. A. Palacios, A. J. Mota, J. Ruiz, M. M. Hänninen, R. Sillanpää, E. Colacio, *Inorg. Chem.* **2012**, *51*, 7010–7012; d) T. D. Pasatoiu, C. Tiseanu, A. M. Madalan, B. Jurca, C. Duhayon, J. P. Sutter, M. Andruh, *Inorg. Chem.* **2011**, *50*, 5879–5889; e) H. Wang, H. Ke, S.-Y. Lin, Y. Guo, L. Zhao, J. Tang, Y.-H. Li, *Dalton Trans.* **2013**, *42*, 5298–5303; f) K. Xiong, X. Wang, F. Jiang, Y. Gai, W. Xu, K. Su, X. Li, D. Yuan, M. Hong, *Chem. Commun.* **2012**, *48*, 7456–7458.

[5] a) M. Andruh, I. Ramade, E. Codjovi, O. Guillou, O. Kahn, J. C. Trombe, *J. Am. Chem. Soc.* **1993**, *115*, 1822–1829; b) C. Aronica, G. Pilet, G. Chastanet, W. Wernsdorfer, J.-F. Jacquot, D. Luneau, *Angew. Chem. Int. Ed.* **2006**, *45*, 4659–4662; *Angew. Chem.* **2006**, *118*, 4775–4778; c) V. Baskar, K. Gopal, M. Helliwell, F. Tuna, W. Wernsdorfer, R. E. P. Winpenny, *Dalton Trans.* **2010**, *39*, 4747–4750; d) V. Chandrasekhar, A. Dey, S. Das, M. Rouzières, R. Clérac, *Inorg. Chem.* **2013**, *52*, 2588–2598; e) J.-P. Costes, J. M. Clemente-Juan, F. Dahan, J. Milon, *Inorg. Chem.* **2004**, *43*, 8200–8202; f) J.-P. Costes, F. Dahan, W. Wernsdorfer, *Inorg. Chem.* **2006**, *45*, 5–7; g) H. L. C. Feltham, R. Clérac, A. K. Powell, S. Brooker, *Inorg. Chem.* **2011**, *50*, 4232–4234; h) O. Iasco, G. Novitchi, E. Jeanneau, W. Wernsdorfer, D. Luneau, *Inorg. Chem.* **2011**, *50*, 7373–7375; i) M. L. Kahn, C. Mathonière, O. Kahn, *Inorg. Chem.* **1999**, *38*, 3692–3697; j) S. K. Langley, L. Ungur, N. F. Chilton, B. Moubaraki, L. F. Chibotaru, K. S. Murray, *Chem. Eur. J.* **2011**, *17*, 9209–9218; k) F. Mori, T. Nyui, T. Ishida, T. Nogami, K.-Y. Choi, H. Nojiri, *J. Am. Chem. Soc.* **2006**, *128*, 1440–1441; l) G. Novitchi, J.-P. Costes, J.-P. Tuchagues, L. Vendier, W. Wernsdorfer, *New J. Chem.* **2008**, *32*, 197–200; m) G. Novitchi, W. Wernsdorfer, L. F. Chibotaru, J.-P. Costes, C. E. Anson, A. K. Powell, *Angew. Chem. Int. Ed.* **2009**, *48*, 1614–1619; *Angew. Chem.* **2009**, *121*, 1642–1647; n) A. Okazawa, T. Nogami, H. Nojiri, T. Ishida, *Chem. Mater.* **2008**, *20*, 3110–3119; o) S. Osa, T. Kido, N. Matsumoto, N. Re, A. Pochaba, J. Mrozinski, *J. Am. Chem. Soc.* **2004**, *126*, 420–421; p) J.-P. Sutter, M. L. Kahn, O. Kahn, *Adv. Mater.* **1999**, *11*, 863–865; q) Q. Zhu, S. Xiang, T. Sheng, D. Yuan, C. Shen, C. Tan, S. Hu, X. Wu, *Chem. Commun.* **2012**, *48*, 10736–10738.

[6] a) G. Christou, D. Gatteschi, D. N. Hendrickson, R. Sessoli, *MRS Bull.* **2000**, *25*, 66–71; b) D. J. Price, S. R. Batten, B. Moubaraki, K. S. Murray, *Chem. Commun.* **2002**, 762–763; c) E. C. Sañudo, W. Wernsdorfer, K. A. Abboud, G. Christou, *Inorg. Chem.* **2004**, *43*, 4137–4144; d) E. K. Brechin, M. Soler, G. Christou, J. Davidson, D. N. Hendrickson, S. Parsons, W. Wernsdorfer, *Polyhedron* **2003**, *22*, 1771–1775; e) E. K. Brechin, M. Soler, G. Christou, M. Helliwell, S. J. Teat, W. Wernsdorfer, *Chem. Commun.* **2003**, 1276–1277; f) H. Miyasaka, R. Clérac, W. Wernsdorfer, L. Lecren, C. Bonhomme, K.-i. Sugiura, M. Yamashita, *Angew. Chem. Int. Ed.* **2004**, *43*, 2801–2805; *Angew. Chem.* **2004**, *116*, 2861–2865; g) H. Miyasaka, T. Nezu, K. Sugimoto, K.-i. Sugiura, M. Yamashita, R. Clérac, *Chem. Eur. J.* **2005**, *11*, 1592–1602; h) L. Lecren, W. Wernsdorfer, Y.-G. Li, O. Roubeau, H. Miyasaka, R. Clérac, *J. Am. Chem. Soc.* **2005**, *127*, 11311–11317; i) C. Kachi-Terajima, H. Miyasaka, K.-i. Sugiura, R. Clérac, H. Nojiri, *Inorg. Chem.* **2006**, *45*, 4381–4390; j) C. Kachi-Terajima, H. Miyasaka, A. Saitoh, N. Shirakawa, M. Yamashita, R. Clérac, *Inorg. Chem.* **2007**, *46*, 5861–5872; k) V. Mereacre, A. M. Ako, R. Clérac, W. Wernsdorfer, I. J. Hewitt, C. E. Anson, A. K. Powell, *Chem. Eur. J.* **2008**, *14*, 3577–3584; l) M. Li, Y. Lan, A. M. Ako, W. Wernsdorfer, C. E. Anson, G. Buth, A. K. Powell, Z. Wang, S. Gao, *Inorg. Chem.* **2010**, *49*, 11587–11594.

[7] a) A. N. Georgopoulou, Y. Sanakis, A. K. Boudalis, *Dalton Trans.* **2011**, *40*, 6371–6374; b) R. F. Weinland, A. Herz, *Ber. Dtsch. Chem. Ges.* **1912**, *45*, 2662–2680; c) F. E. Sowrey, C. Tilford, S. Wocadlo, C. E. Anson, A. K. Powell, S. M. Bennington, W. Montfrooij, U. A. Jayasooriya, R. D. Cannon, *Dalton Trans.* **2001**, 862–866; d) C. J. Milios, M. Manoli, G. Rajaraman, A. Mishra, L. E. Budd, F. White, S. Parsons, W. Wernsdorfer, G. Christou, E. K. Brechin, *Inorg. Chem.* **2006**, *45*, 6782–6793.

[8] R. E. P. Winpenny, *Dalton Trans.* **2002**, 1–10.

[9] M. N. Akhtar, Y. Lan, V. Mereacre, R. Clérac, C. E. Anson, A. K. Powell, *Polyhedron* **2009**, *28*, 1698–1703.

[10] M. N. Akhtar, Y.-Z. Zheng, Y. Lan, V. Mereacre, C. E. Anson, A. K. Powell, *Inorg. Chem.* **2009**, *48*, 3502–3504.

[11] A. M. Ako, V. Mereacre, R. Clérac, I. J. Hewitt, Y. Lan, G. Buth, C. E. Anson, A. K. Powell, *Inorg. Chem.* **2009**, *48*, 6713–6723.

[12] V. Mereacre, A. M. Ako, M. N. Akhtar, A. Lindemann, C. E. Anson, A. K. Powell, *Helv. Chim. Acta* **2009**, *92*, 2507–2524.

[13] V. Mereacre, M. N. Akhtar, Y. Lan, A. M. Ako, R. Clérac, C. E. Anson, A. K. Powell, *Dalton Trans.* **2010**, *39*, 4918–4927.

[14] W. Liu, H. H. Thorp, *Inorg. Chem.* **1993**, *32*, 4102–4105.

[15] a) L. Vilà-Nadal, L. Cronin, *Nat. Rev. Mater.* **2017**, *2*, 17054; b) S. Zhao, T. Gensch, B. Murray, Z. L. Niemeyer, M. S. Sigman, M. R. Biscoe, *Science* **2018**, *362*, 670; c) F. Peiretti, J. M. Brunel, *ACS Omega* **2018**, *3*, 13263–13266; d) M. K. Nielsen, D. T. Ahneman, O. Riera, A. G. Doyle, *J. Am. Chem. Soc.* **2018**, *140*, 5004–5008; e) D. T. Ahneman, J. G. Estrada, S. Lin, S. D. Dreher, A. G. Doyle, *Science* **2018**, *360*, 186; f) J. P. Reid, M. S. Sigman, *Nature* **2019**, *571*, 343–348; g) S. H. M. Mehr, M. Craven, A. I. Leonov, G. Keenan, L. Cronin, *Science* **2020**, *370*, 101.

[16] a) D. Caramelli, J. Granda, H. Mehr, D. Cambié, A. Henson, L. Cronin, *ChemRxiv.* **2021**, DOI: 10.26434/chemrxiv.12924968.v2; b) V. Duros, J. Grizou, W. Xuan, Z. Hosni, D.-L. Long, H. N. Miras, L. Cronin, *Angew. Chem. Int. Ed.* **2017**, *56*, 10815–10820; *Angew. Chem.* **2017**, *129*, 10955–10960; c) L. J. Points, J. W. Taylor, J. Grizou, K. Donkers, L. Cronin, *Proc. Nat. Acad. Sci.* **2018**, *115*, 885; d) T. Minato, D. Salley, N. Mizuno, K. Yamaguchi, L. Cronin, K. Suzuki, *J. Am. Chem. Soc.* **2021**, *143*, 12809–12816.

[17] V. M. Mereacre, A. M. Ako, R. Clérac, W. Wernsdorfer, G. Filoti, J. Bartolomé, C. E. Anson, A. K. Powell, *J. Am. Chem. Soc.* **2007**, *129*, 9248–9249.

[18] G. M. Sheldrick, *Acta Crystallogr A Found. Adv.* **2015**, *71*, 3–8.

[19] G. M. Sheldrick, *Acta Crystallogr C Struct Chem* **2015**, *71*, 3–8.

[20] O. V. Dolomanov, L. J. Bourhis, R. J. Gildea, J. A. K. Howard, H. Puschmann, *J. Appl. Crystallogr.* **2009**, *42*, 339–341.

Supporting Information

Experimental details

$[Mn_6O_2(piv)_{10}(4\text{-Me-py})_2(pivH)_2]$ (1). Compound **1** was obtained as previously reported in Reference [18].

$[Mn_7Nd_3(O)_4(OH)_4(mdea)_3(piv)_9(NO_3)_3]\cdot 3MeCN$ (2). $Nd(NO_3)_3\cdot 6H_2O$ (0.29 g, 0.66 mmol) was added to a stirred slurry of **1** (0.20 g, 0.11 mmol) and *N*-methyldiethanolamine (0.140 g, 1.17 mmol) in MeCN (15 ml). After stirring for 5 minutes at room temperature, the mixture was heated at ~ 70°C for 35 minutes to give a dark-brown solution. The solution was allowed to cool, filtered, and left to evaporate slowly at room temperature in a 25 ml glass covered with parafilm. Dark brown crystals were obtained after one week, collected by filtration, washed with 5 ml cold MeCN, and dried in air. Yield: 65 mg (27.0 % based on Mn). Elemental analysis calcd (%) for $C_{60}H_{118}N_6O_{41}Mn_7Nd_3$ (dried): C 30.06, H 4.96, N 3.50; found: C 29.93, H 5.07, N 3.34. IR (KBr): ν/cm^{-1} = 3419 (b, m), 2962 (s), 2929 (s), 2871 (s), 1608 (vs), 1564 (s), 1548 (s), 1484 (vs), 1463 (s), 1408 (vs), 1372 (s), 1358 (s), 1282 (s), 1223 (s), 1068 (s), 1027 (w), 996 (m), 903 (w), 816 (w), 794 (w), 758 (w), 736 (w), 682 (w), 632 (s), 614 (s), 549 (m), 460 (w).

Compounds 3 and **4:** were obtained by the same procedure using $Sm(NO_3)_3\cdot 6H_2O$ and $Eu(NO_3)_3\cdot 6H_2O$ respectively in place of $Nd(NO_3)_3\cdot 6H_2O$. Their IR spectra are similar.

$[Mn_7Sm_3(O)_4(OH)_4(mdea)_3(piv)_9(NO_3)_3]\cdot 3MeCN$ (3). Yield: 60 mg (25.0 % based on Mn). Anal. calc. for $C_{60}H_{118}Mn_7N_6O_{41}Sm_3$ (dried): C 29.84, H 4.92, N 3.48; found: C 29.66, H 4.99, N 3.37.

$[Mn_7Eu_3(O)_4(OH)_4(mdea)_3(piv)_9(NO_3)_3]\cdot 3MeCN$ (4). Yield: 62 mg (25.8 % based on Mn). Anal. calc. for $C_{60}H_{118}Eu_3Mn_7N_6O_{41}$ (dried): C 29.78, H 4.91, N 3.47; found: C 29.57, H 5.03, N 3.34.

$[Mn_7Gd_3(O)_4(OH)_4(mdea)_3(piv)_9(NO_3)_3]\cdot 3MeCN$ (5). For this compound the same synthetic procedure as above was used with small changes: after the solution was left for the evaporation, after one day it was again filtered to removed any brown crystals of the starting material, Mn_6 (**1**). The filtrate was covered again with parafilm and left for further crystallization. After one week new, darker crystals were formed and filtered off. This product was tested to be compound **5**. Yield: 25 mg (10.4 % based on Mn). Anal. Calcd for $C_{60}H_{118}Gd_3Mn_7N_6O_{41}$ (dried): C 29.58, H 4.88, N 3.45; found: C 29.39, H 4.97, N 3.41.

If the filtrate from the second filtration is left for further crystallization, then a batch of crystals is obtained which is a mixture of two new compounds $[Mn_5Gd_4(O)_6(mdea)_2(mdeaH)_2(piv)_6(NO_3)_4(H_2O)_2]\cdot 2MeCN$ (**6**) and $[Mn_2Gd_2(OH)_2(mdeaH)_2(piv)_6(NO_3)_2]\cdot MeCN$ (**7**) (Figure 2). These crystals can be separated from each other on the basis of their colour: pale orange (**7**) or black (**6**). Yield: 25 mg (10.4 % based on Mn). Anal. Calcd for $C_{42}H_{83}N_5O_{24}Gd_2Mn_2$ (dried): C 34.35, H 5.70, N 4.77; found: C 31.56, H 5.11, N 4.60.

Compounds 8-9: $[Mn_2Ln_2(OH)_2(mdeaH)_2(piv)_6(NO_3)_2]$ (Ln = Pr (**8**), Nd (**9**) can be isolated using the same synthetic procedure as above but using a 1:1 mixture of MeOH and MeCN instead of MeCN as a solvent. Anal. Calcd for $C_{42}H_{83}N_5O_{24}Pr_2Mn_2$ (dried): C 35.17, H 5.84, N 4.89; found: C 29.66, H 4.77, N 4.13. Anal. Calcd for $C_{42}H_{83}N_5O_{24}Nd_2Mn_2$ (dried): C 35.12, H 5.83, N 4.88; found: C 29.91, H 4.70, N 3.52

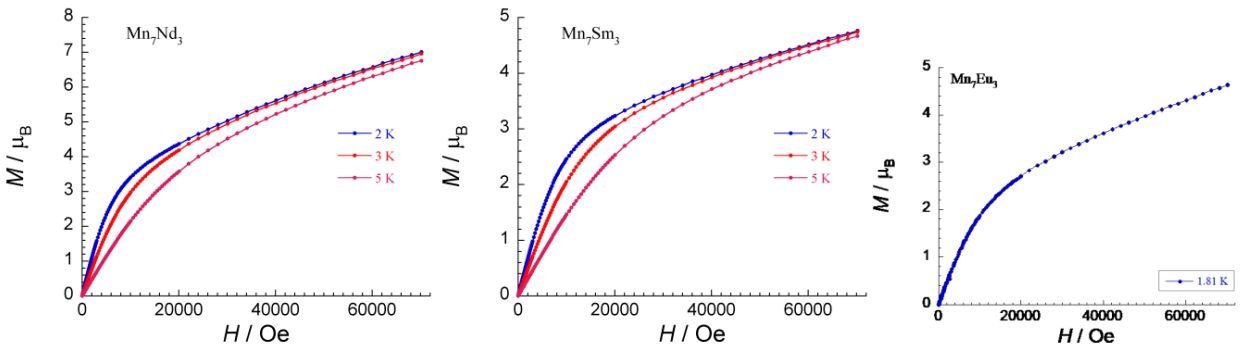

Figure S1. Field dependence of the magnetization for **2-4**.

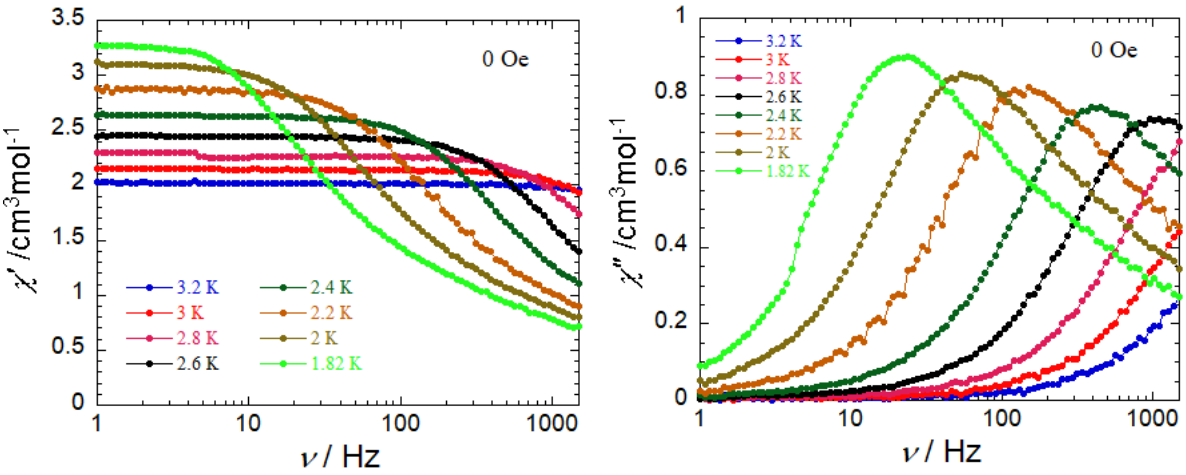

Figure S2. Frequency dependence of the in-phase, χ', left, and out-of-phase, χ", right, components of the ac magnetic susceptibility obtained for **2** in zero dc applied field for frequencies 1 – 1500 Hz.

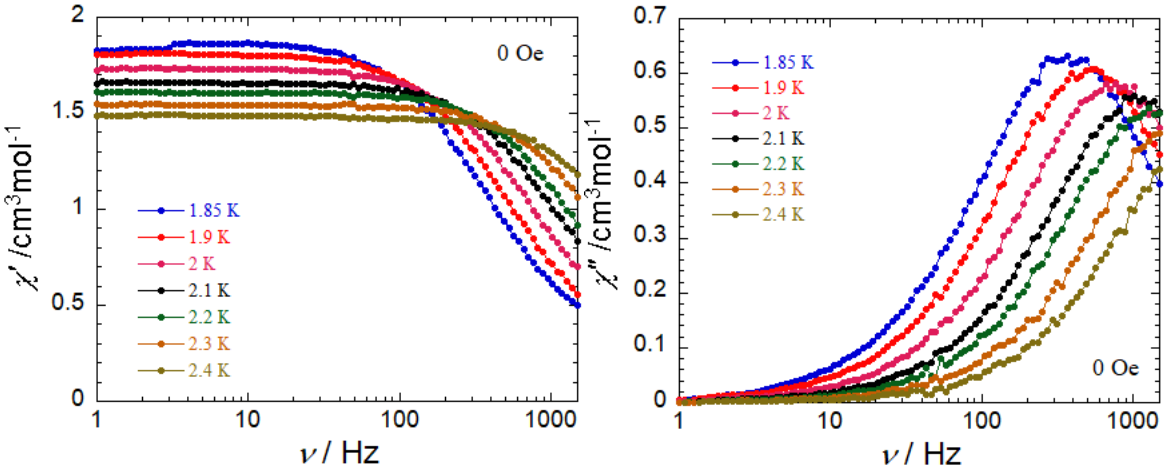

Figure S3. Frequency dependence of the in-phase, χ', left, and out-of-phase, χ", right, components of the ac magnetic susceptibility obtained for **3** in zero dc applied field for frequencies 1 – 1500 Hz.

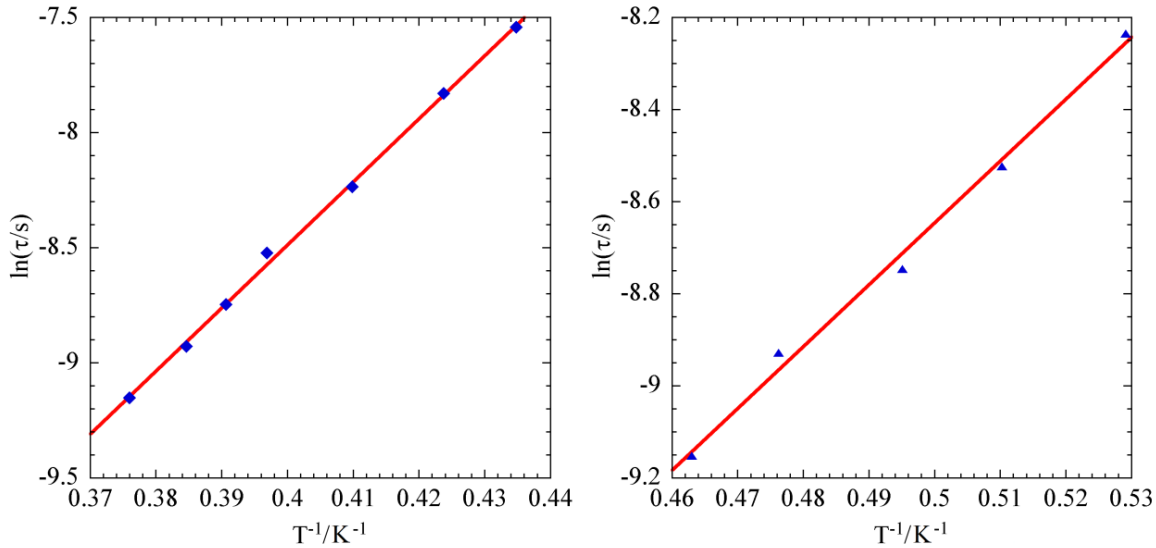

Figure S4. ln(τ) vs T^{-1} plots for **2** (left) and **3** (right).

Table S1 unit cell parameters for compounds **5** and **7-9**, the unit cell for compound **2** is listed for comparison

	2	**5**	**7**	**8**	**9**
Formula	$C_{66}H_{127}Mn_7N_9Nd_3O_{41}$	$C_{66}H_{127}Mn_7N_9Gd_3O_{41}$	$C_{42}H_{83}Mn_2N_5Gd_2O_{24}$	$C_{44}H_{86}Mn_2N_6Pr_2O_{24}$	$C_{44}H_{86}Mn_2N_6Nd_2O_{24}$
Mr	2520.07	2559.08	1466.51	1474.88	1474.88
crystal system	triclinic	triclinic	monoclinic	monoclinic	monoclinic
space group	P-1	P-1	P-1	P-1	P-1
a [Å]	14.3815(11)	14.320(2)	10.9664(7)	10.9078(4)	10.9783(3)
b [Å]	15.0511(11)	14.958(2)	14.0196(9)	13.3251(5)	13.9773(4)
c [Å]	25.8828(19)	25.736(3)	21.8482(14)	13.7408(5)	21.8074(5)
α [°]	91.889(1)	91.692(2)	78.567(5)	100.104(3)	78.5170
β [°]	100.900(1)	101.228(2)	79.212(5)	112.766(3)	79.2730
γ [°]	111.755(1)	111.819(2)	68.444(5)	111.712(3)	68.5000
V [Å^3]	5076.9(7)	4988(2)	3037.2	1588.23(11)	3027.5
Z	2	2	2	1	2

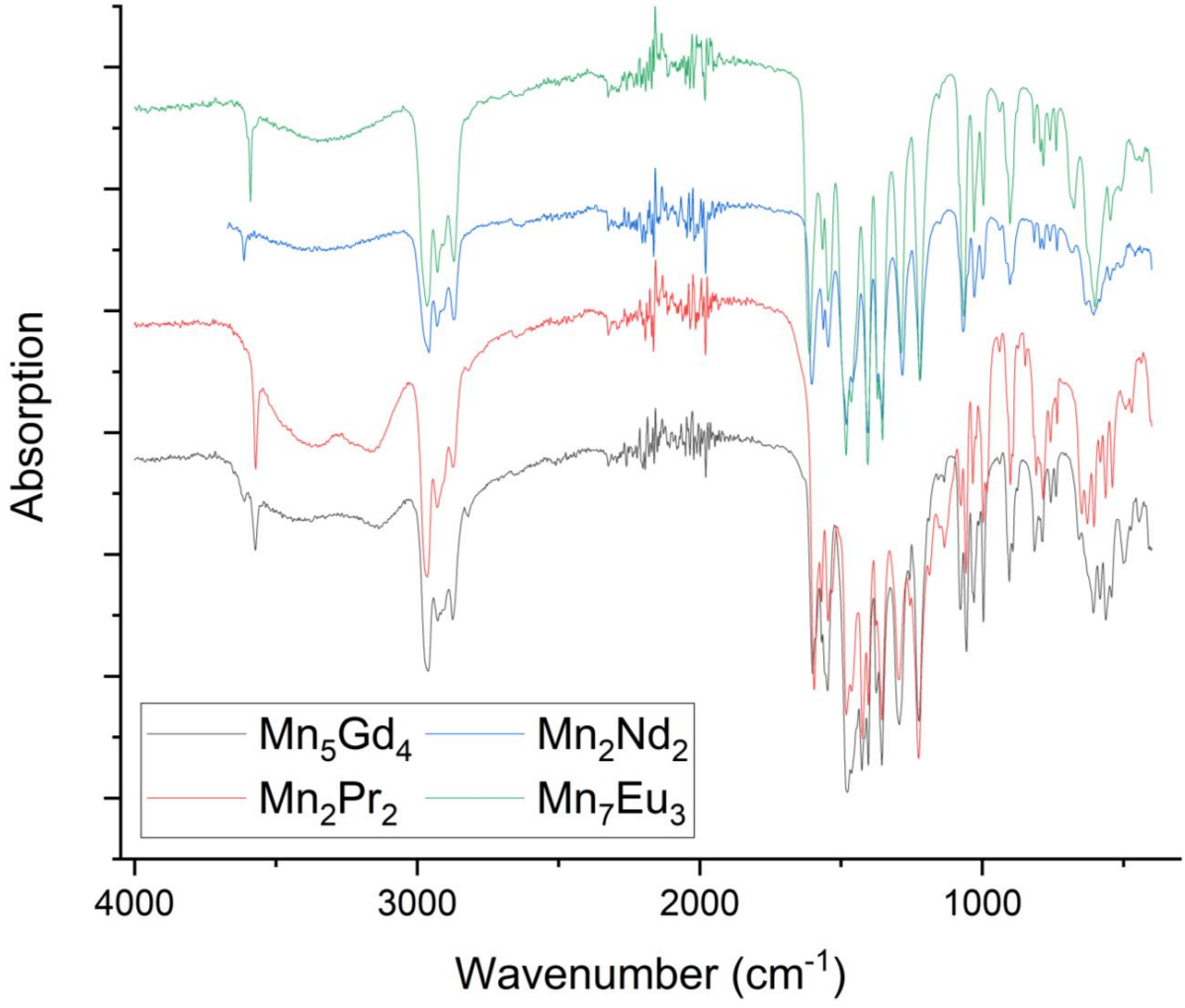

Figure S5 IR spectra of Mn_7Eu_3 (**4**) Mn_5Gd_4 (**5**) Mn_2Nd_2 (**8**) and Mn_2Pr_2 (**9**) stacked for better visibility. The spectra are virtually identical

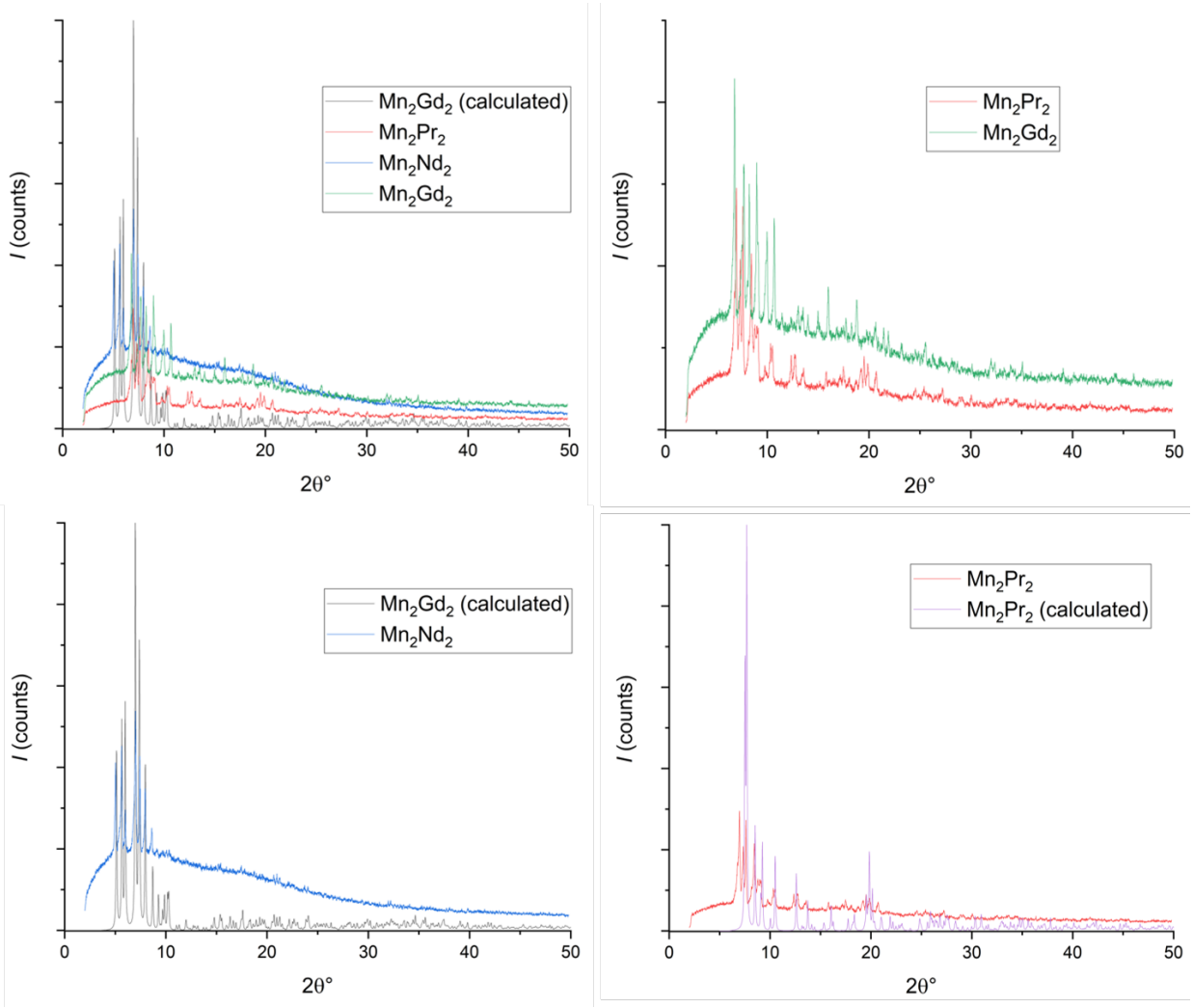

Figure S6 PXRDs of compounds 7-9 and calculated powder patterns for the two unit cells for these compounds

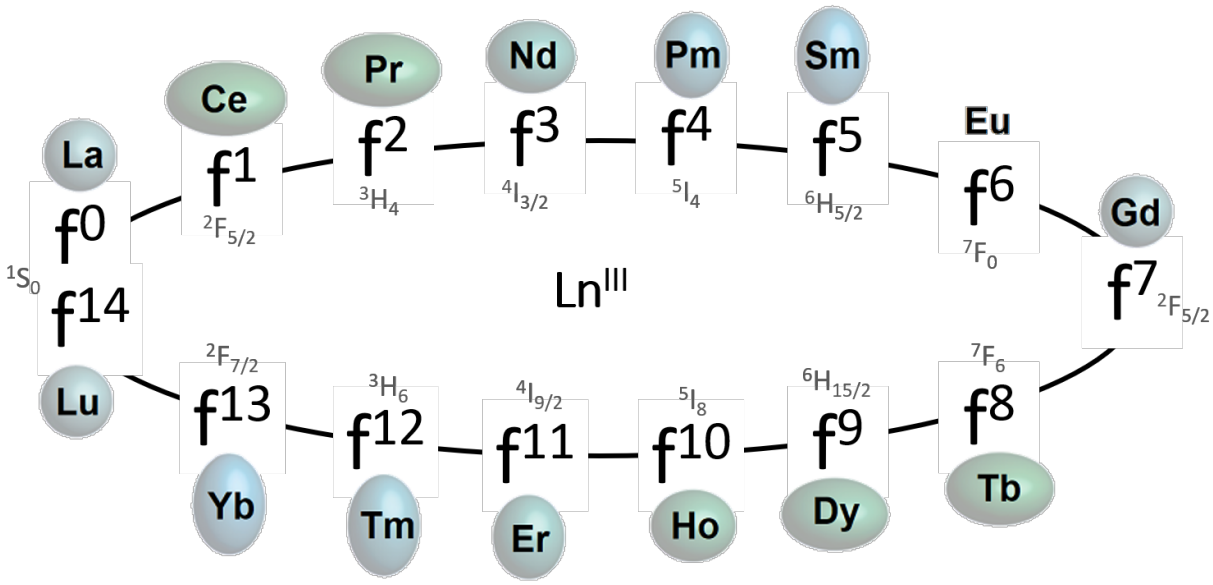

Figure S7 The cyclic relationship within the Ln-series showing the opposite shape of the electron density ellipsoids for lanthanides with the same amount of unpaired f electrons, of particular interest to this manuscript is the inverse relationship between Sm-Dy and Nd-Er.